Твердотельная электроника

UDC 53.097

I. Brodnikovska, Ph.D.
Frantsevich Institute for Problems of Materials Science of NASU,
Krzhizhanovsky str. 3, 03680, Kyiv, Ukraine

Characterization of SOFC electrolytes using impedance spectroscopy analysis (overview)

The overview paper considers the difference of electrical characterization methods for the electrodes and electrolytes of SOFC. Features of the use of IS for SOFC electrolytes with Debye response was shown. A comprehensive study of possible non-Debye relaxation mechanisms in SOFC materials was made. The definition of microstructure parameters in the case of non-Debye representation was shown on the example of experimental study of 10Sc1CeSZ ceramics. Ref. 22, Fig. 8, Tables 2.

Keywords: *solid oxide fuel cell (SOFC); electrolyte; electrical characterization; impedance spectroscopy; Debye and non-Debye responses.*

1. Introduction. What is a solid oxide fuel cell?

Fuel cells are the devices which produce electricity and heat from electrochemical reaction of hydrogen and/or carbon monoxide fuel with oxygen. Unlike Carnot engines, they do not burn the fuel so they are tend to be more efficient (≈ 54 up to 62 % [1]) and cleaner. A fuel cell usually contains an electrolyte places between two electrodes with connectors for collecting the generated current. Fuel cell technology produces clean, efficient, reliable electrical power to almost any device requiring it [2].

SOFCs (solid oxide fuel cells) use a solid oxide electrolyte to conduct negative oxygen ions from the cathode to the anode. A typical solid oxide fuel cell, which essentially consists of two porous electrodes, separated by a dense, oxide ion conducting electrolyte, is shown in Fig. 1.

Oxygen gas molecules on the cathode react with the incoming electrons from the external circuit to form oxide ions, which then migrate through the oxide ion–conducting electrolyte to the anode. At the anode, the oxide ions react with the fuel to form water (and/or carbon dioxide), liberating electrons, which flow from the anode through the external circuit to the cathode to produce electricity. Due to continuous supply by fuel and oxygen, these electrochemical reactions generate electricity continuously [3].

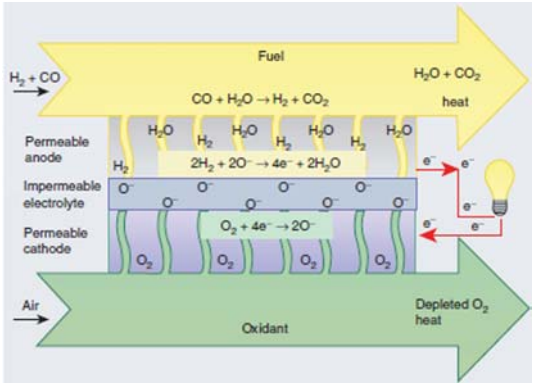

Fig. 1. Operating principle of a solid oxide fuel cell (SOFC) [3]

1.1. SOFC components and methods of their electrical characterization

For maximization of the active reaction area and hence a lowering of the polarization resistance, SOFC electrodes consists today of interpenetrating ionically and electronically conducting networks. This can be achieved by the use of mixed ionic electronic conductor (MIEC) materials or composite electrodes where one material is a good electronic conductor and the other material a good oxide ion conductor [4]. Currently, Ni-yttria stabilized zirconia (YSZ) cermet is the most commonly used anode material [3], lanthanum strontium manganite (LSM)-YSZ – the cathode [4].

Electrochemical impedance spectroscopy (EIS, IS) has proven itself as a powerful losses monitoring technique within a SOFC, and also it provides the understanding which component and/or process first degrade under operation. According to [4] usually the impedance diagrams of SOFC electrodes has been estimated using traditional approximation based on a series of suppressed semicircles, each of which is then usually ascribed to a specific reaction or process. However, an application of such an approach for electrodes often is not valid because the processes can be coupled: for example, diffusion followed by reaction, gas diffusion coupled with gas conversion in anodes, cou-

pling between diffusion and reaction. The authors [4] showed that the impedance response of such systems can be successfully described by porous electrode theory (PET) [5]. The structure of a porous electrode is modeled in PET as cylindrical pores containing the electrolyte, while the pore wall corresponds to the surface of the solid electronically conducting electrode. The structure of SOFC composite electrodes e.g. LSM:YSZ can be modeled as YSZ columns surrounded by the LSM electrocatalyst as illustrated in Fig. 2A [4]. The classic composite Ni:YSZ cermet SOFC anode can be modeled analogically by replacing LSM with Ni [6]. The coupling between the impedance of the percolated conducting networks χ_1 and χ_2 and the impedance of the electrochemical reaction ζ can be described by the general transmission line depicted to the left in Fig. 2.

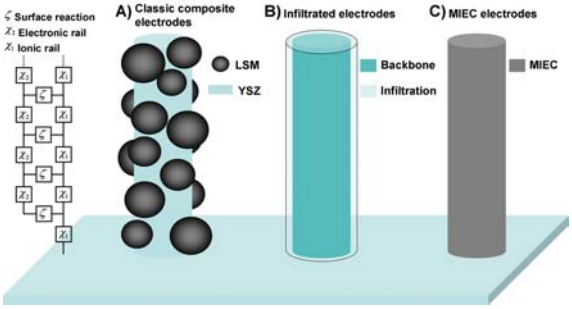

Fig. 2. Transmission line describing the various SOFC electrode models: A) model of classic composite electrodes. In this particular case the LSM:YSZ composite cathode; B) model of an infiltrated electrode; C) model of a mixed ionic electronic conductor (MIEC) material based cathode [4]

Typical electrolyte materials for SOFCs are oxides with low valence element substitutions, which create oxygen vacancies (acceptor dopants) through charge compensation [3]. The most common materials of SOFC electrolytes are zirconium oxide, stabilized by yttria [7], scandia [8] and ceria [9]. Various alloying additives (for example, Bi_2O_3, YbO_3, Mn_2O_3, Ga_2O_3 and Al_2O_3) are used to ensure the stability of required phase transitions.

Concerning the electrical characterization of solid electrolytes, the electrical impedance spectroscopy is frequently used to separate the different contributions to the electrical resistivity [10]. This paper consider the use of IS for electrical characterization of SOFC electrolytes.

1.2. Debye and non-Debye relaxation mechanisms in SOFC materials

The representation of the AC electrical data in the complex plane display two general types of processes known as ideal (Debye) and non-ideal (non-Debye) types [11]. The ideal or Debye relaxation process is observed only in polar liquids. It is attributed to dipole polarization. The Debye behavior is represented in the form of the semicircular response in the complex plane formalism the center of which lies on the real axis (*x*-axis). The other response (non-Debye type) can be observed via the skewed behavior of the semicircular curve or its depression of real axis. It is well-known [10,11] that in solid materials with ionic polarization dielectric responses are often described as Cole-Cole (C-C), Davidson-Cole (D-C) and Havriliak-Negami (H-N) relaxations in the complex plane formalism. But, unfortunately, most of today's works elide this aspect of matter. Thereby we have not enough information concerning relaxation parameters. In present work we have made a comprehensive study of possible non-Debye relaxation mechanisms in SOFC materials.

2. Structural analysis of SOFC components' conductivity in the case of Debye representation

If the complex dielectric permittivity is given by the Debye's equation (1)

$$\varepsilon^*(\omega) = \varepsilon_\infty + \frac{\varepsilon_0 - \varepsilon_\infty}{1 + j\omega\tau} = \varepsilon' - j\varepsilon'', \qquad (1)$$

where ε_∞ - permittivity at ultra high frequencies, ε - effective value of permittivity (at $f \to 0$ Hz, τ - relaxation time, than real and imaginary parts of impedance in $Z'(Z'')$ coordinates give ideal semicircle with the centre on the real axis. In such case methods of impedance spectroscopy easily allow to separate the contributions of the different phases and components to the electrical resistance of the system.

In the case of two-phase insulator-conductor medium with dielectric matrix there are two arcs on the complex plane, each of which characterizes the contribution of one component: grain contribution at high frequency (HF) and grain boundary phase at low frequency (LF) (associated with the accumulation of charge carriers on the grains' surface) (Fig. 3, a). This is evidenced by the fact that in ytria-stabiled zirconia with dielectric additives such as aluminium oxide additives [12] or structure defects like pores [13], the largest feedback occurred in LF arc.

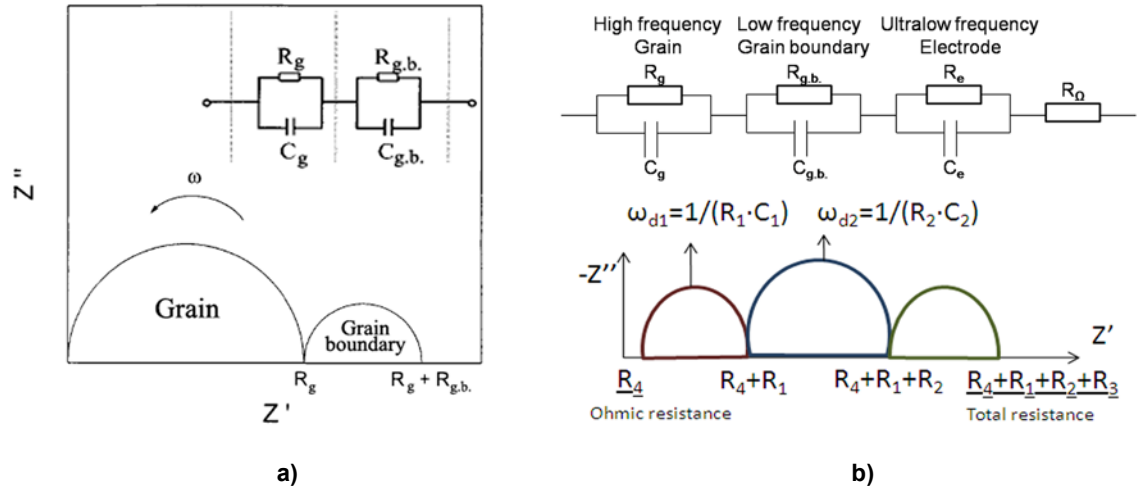

Fig. 3. Schematic impedance diagrams and the corresponding equivalent schemes of: a) polycrystalline (ceramic) samples; b) polycrystalline (ceramic) samples with contact's contribution

Some reports [15] also showed the ultralow frequency contribution due to reactions on the electrodes surface (Fig. 3, b). In this case real and imaginary parts of impedance are described as follows:

$$Z' = \frac{R_1}{1+(\omega C_1 R_1)^2} + \frac{R_2}{1+(\omega C_2 R_2)^2} + \frac{R_3}{1+(\omega C_3 R_3)^2} + R_4, \quad (2)$$

$$Z'' = -\left(\frac{\omega C_1 R_1^2}{1+(\omega C_1 R_1)^2} + \frac{\omega C_2 R_2^2}{1+(\omega C_2 R_3)^2} + \frac{\omega C_3 R_3^2}{1+(\omega C_3 R_3)^2}\right). \quad (3)$$

2.1. Effect of alumina on the properties of ceria and scandia co-doped zirconia studied by IS

It is well known that the grain-boundary resistance usually has the largest contribution to total resistance of the electrolyte sample due to its defect structure. Earlier studies have shown that the silicon-rich amorphous phases are the most common reason for [15] it. As SiO_2 in ceramic technology is practically unavoidable impurity, it is difficult to be excluded even in sample prepared with high grade powders. It has been found that the grain boundary resistance of YSZ can be reduced significantly by the addition of additives such as La_2O_3, Bi_2O_3, and Al_2O_3 [16-18].

Thus the effect of alumina on conductivity of SCSZ was evaluated for electrolyte-supported SOFC application [19].

Different composites of SCSZ/Al_2O_3 with compositions of 0, 0.25, 1, 2 and 5 wt% of alumina were prepared (denoted as A00, A02, A05, A10, A20, and A50, respectively).

Impedance spectra (Fig. 4) showed that small addition (up to 0.5 wt%) of alumina had little influence on the bulk (grain interior) resistance. The bulk resistances of A00, A02 and A05 were 80.4, 80.6, 81.0 kΩ cm, respectively, increasing slightly with increasing alumina content. However, a much stronger decrease was observed in grain boundary resistivity, causing the decrease in the total resistance of composites.

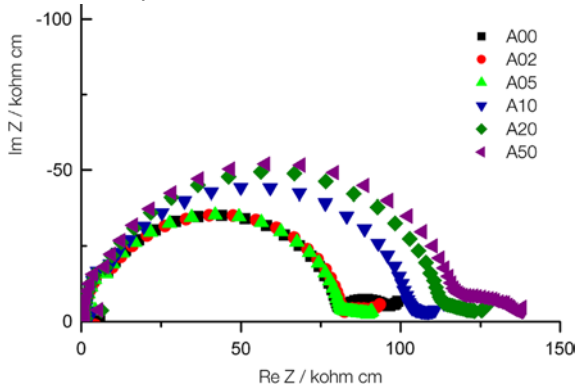

Fig. 4. Impedance spectra of SCSZ/Al_2O_3 samples measured at 350 °C [Ошибка! Закладка не определена.**]**

Higher alumina content caused a pronounced increase in bulk and grain boundary resistances. Thus, it was shown that aluminium oxide in an amount of up to 1 wt% is effective sintering additive which promotes the stabilization at cubic phase and reduces resistance of grain boundary phase.

2.2. IS study of electrical degradation in electrolytes

Commercially viable SOFC electrolytes should possess not only high ionic conductivity but also minimal conductivity degradation at operating temperatures. It has been stated that, for the degradation of electrolyte conductivity has to be less than

0.1% per 1000 h [20]. On this reason, the long-term conductivity stability was tested on zirconia based electrolyte materials [21]. The ageing studies have been performed on the samples of ZrO_2 co-doped with 10 mol% of Sc_2O_3 and 1 mol% MO_2, where M = Ce or Hf (denoted respectively 1Ce10ScSZ and 1Hf10ScSZ) in oxidizing and reducing atmospheres, at 600 °C for 3000 h.

Authors argued that due to the high relaxation frequency of the grain at 600 °C and inductance from the experimental set-up, the semicircle due to the intra-grain polarization was not observed (Fig. 5). The intermediate semicircle was due to the grain boundary polarization (on their opinion it was confirmed by its capacitance value ~$1.9 \cdot 10^{-8}$ F/cm). Thus, only the grain boundary semi-circle and low-frequency electrode arc were observed in the plot.

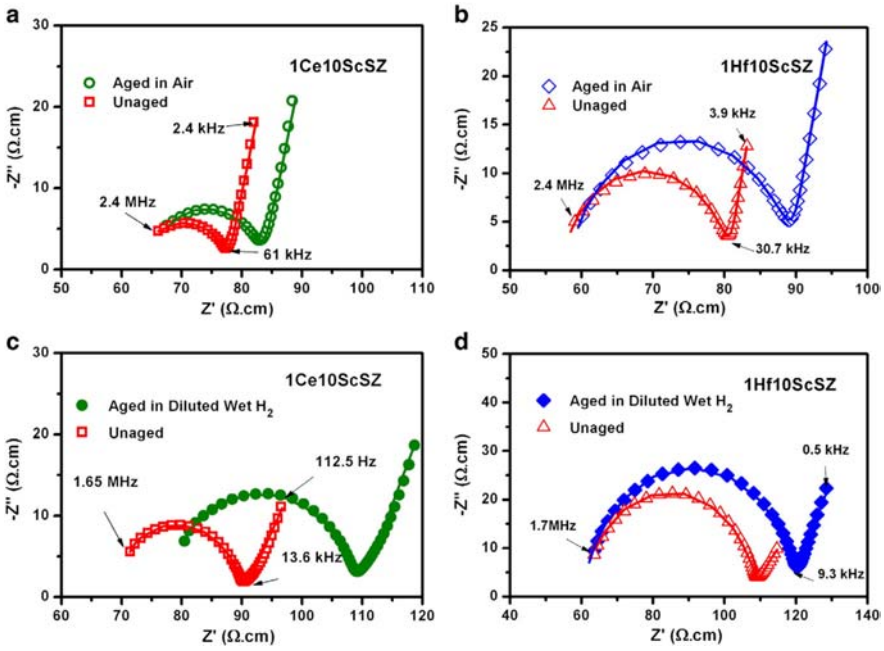

Fig. 5. Impedance plot for 1Ce10ScSZ samples before and after ageing in a) air and in c) reducing conditions at 600 °C for 3000 h. Impedance spectrum for 1Hf10ScSZ samples before and after ageing in b) air and in d) reducing conditions are also shown [21]

It was shown that after the ageing process in both the compositions, the grain boundary semicircle becomes larger than in the unaged samples, indicating the increase in the grain boundary resistivity. The loss of conductivity in air is lower than in reducing conditions. For 1Ce10ScSZ sample aged in reducing conditions, there is a large shift in the grain boundary polarization semicircle towards the higher real impedance value. However, no such large shift was observed for 1Ce10ScSZ and 1Hf10ScSZ samples aged in air. Similar is the case in the impedance plot of 1Hf10ScSZ sample aged in reducing conditions. The shift in the grain boundary polarization semicircle is suggestive of the increase in the grain resistivity in the sample. Thus, the 1Ce10ScSZ sample aged in reducing conditions exhibited higher increase in the grain resistivity (the highest degradation rate of 3.8%/1000 h) compared to the ageing in air or 1Hf10ScSZ composition.

But in spite of the authors' point of view [21], the semicircle between 1-2 MHz and 10 kHz is rather belonging to grain response, the "tail" is the beginning of grain boundary response and unnoticed semicircle due to the intra-grain polarization was just an ohmic resistance. Besides, our experiments (shown later) confirmed that C~$1.9 \cdot 10^{-8}$ F/cm is very closely to the value of the grain capacitance.

3. Structural analysis of SOFC components' conductivity in the case of non-Debye representation

3.1. Features of the Cole-Cole representation

For this type of relaxation the semicircle lies below the *x*-axis giving rise to a depression angle (θ) measured from the point at the left-intercept to the

center of the semicircle (Fig. 6). The Cole-Cole behavior can be expressed as:

$$\varepsilon^*(\omega) = \varepsilon_\infty + \frac{\varepsilon_0 - \varepsilon_\infty}{1 + (j\omega\tau_0)^\alpha}, \quad (1)$$

where the value of α ranges between 0 and 1.

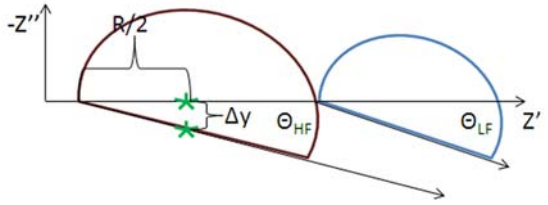

Fig. 6. The generic impedance representation obtained from the Cole-Cole relation

The depression angle can be obtained from Fig. 6 as:

$$\theta = \text{atan}\left(\frac{\Delta y}{R/2}\right). \quad (2)$$

Then the depression parameter *h* is given by:

$$h = \frac{\theta}{\pi/2} = \frac{2\theta}{\pi}. \quad (3)$$

Here parameter (exponent) *α* is related to the depression parameter as:

$$1 - h = \alpha. \quad (4)$$

The ideal Debye or Debye-like behavior can be achieved as $\theta \to 0$ implying $\alpha \to 1$.

3.2. Features of the Davidson-Cole representation

Davidson-Cole empirical equation representing the skewed relaxation curve (Fig. 7) is given by

$$\varepsilon^*(\omega) = \varepsilon_\infty + \frac{\varepsilon_0 - \varepsilon_\infty}{(1 + j\omega\tau_0)^\beta}, \quad (5)$$

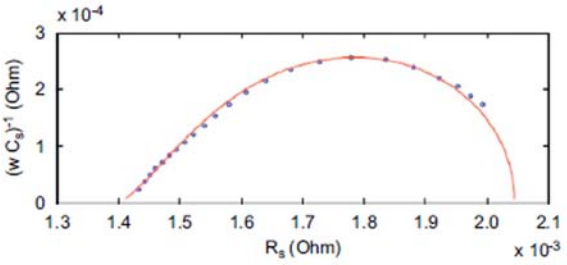

Fig. 7. Davidson-Cole representation of the Ni-Cd battery via impedance plot [11]

For ideal Debye response relaxation time τ_0 is the product of the R-C. Due to the skewed nature of the Davidson-Cole curve, the time constant is not necessarily corresponding to the conventional $\omega\tau = 1$ at the peak. So we considered a scale factor $\frac{Z'_{PF}}{Z''_{PF}}$ or correction for the ideal or Debye relaxation:

$$C = \frac{1}{R\omega_{PF}}\left(\frac{Z'_{PF}}{Z''_{PF}}\right), \quad (6)$$

$$\varphi_{PF} = \arctan\left(\frac{Z'_{PF}}{Z''_{PF}}\right), \quad (7)$$

$$\beta = \frac{\pi}{2\varphi_{PF}} - 1. \quad (8)$$

The parameter β is highly complicated and it reflects perturbation in the relaxation time.

Table 1. Yttria volume fraction and the depression angles β of the fitted intergranular (LF) and intragranular (HF) components of the impedance diagrams [10]

Y_2O_3, mol.%	β_{HF}, °	β_{LF}, °
0	9.5	10.1
1	7.6	11.1
5	8.0	14.7
10	11.7	15.7
20	14.1	17.2
30	-	15.5
50	-	12.1

It is worth to notice that fitting angles θ and β may differ for different semicircles. For example, authors [10] showed that the β values increased with increasing addition of the insulating phase (Table 1). This effect was associated with the higher degree of heterogeneity of the samples with increasing yttria content.

3.3. Havriliak-Negami representation

If the impedance response can be expressed in terms of Havriliak-Negami equation:

$$\varepsilon^*(\omega) = \varepsilon_\infty + \frac{\varepsilon_0 - \varepsilon_\infty}{(1 + (j\omega\tau_0)^\alpha)^\beta}, \quad (9)$$

both α and β parameters can be defined as in previous case.

3.4. Impedance spectroscopy analysis of percolation

The electrical conduction properties of zirconia-based solid electrolytes are largely influenced by the presence of a dispersed second phase or impurities. As a consequence, systematic studies concerning the influence of impurities, and the role played by a dispersed second insulating phase on

bulk and grain boundary transport properties are necessary to better understand the transport mechanisms in zirconia-based solid electrolytes.

The electrical properties of (ZrO_2:8 mol% Y_2O_3) + *m* mol% Y_2O_3 ceramic composites with nominal yttria concentration varying from 0 to 70 mol% (0–82.9 vol%) were studied by impedance spectroscopy (IS) allowing for the separation of the inter- and intragranular components of the electrical conductivity [10].

The dependence of the grain and grain boundary contributions to the electrical conductivity via the insulator content was analyzed according to the general effective medium equation [22]. Results showed good agreement with the experimental data. The percolation thresholds for the total and intergranular contributions were 30 and 27 vol%, respectively while $\sigma(Y_2O_{3content})$ dependence was linearly descending. It was concluded that the percolation threshold for the total electrical conductivity occured at higher (10%) concentrations in relation to the intergranular conductivity which could be associated with the intrinsic blocking of charge carriers at internal surfaces (mainly non-conducting grain boundary regions) of zirconia-based solid electrolytes. Thus authors [10] demonstrated that IS can provide more detailed information about percolation parameters (critical volume fraction and critical exponent) than dc techniques, for systems that exhibit a partial blocking of charge carriers such as stabilized zirconia solid electrolytes.

3.5. Experimental study of 10Sc1CeSZ ceramics

Now let us consider the example of definition of microstructure parameters in the case of non-Debye representation.

Frequency dependences of the real and imaginary part of 10Sc1CeSZ impedance were measured within the frequency range 10^{-2}-10^6 Hz by Solartron 1260 Analyzer. The graph of $-Z''(Z')$ dependence is given on Fig. 8. We can clearly distinguish three semicircles on it: the third one (ultralow frequency) corresponds to the reaction of the electrodes, the second – grain boundary phase, the first (high frequency) – to the grain resistance.

Equations (2) and (3) were used for electrical modeling of the structure. R_1, R_2, R_3, R_4 parameters were found from Figs. 1b, 3. Dispersion frequencies φ_1, φ_2, φ_3 were calculated from (7), as well as capacitances C_1, C_2, C_3 - from (6), depression and skewing parameters α_1, α_2, α_3, θ_1, θ_2, θ_3, β_1, β_2, β_3 - from (2)-(4), (8). Fitting parameters are given in Table 2.

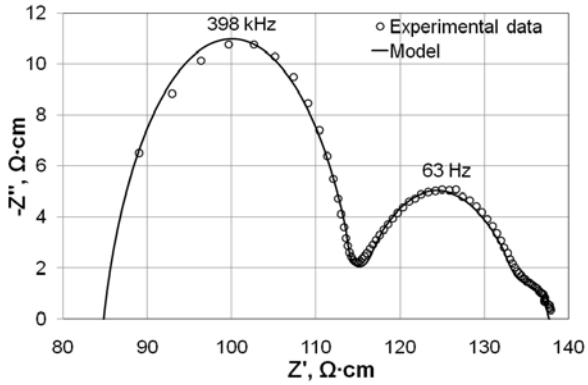

Fig. 8. Impedance diagram of 10Sc1CeSZ ceramics synthesized at 1250 ºC (measurements were provided at 600 ºC). Dots – experimental data, line – result of the modeling

Table 2. Fitting parameters of the model line given in Fig. 3

R_1, Ω·cm	R_2, Ω·cm	R_3, Ω·cm	R_4, Ω·cm
32	26.3	5	84
C_1, F·cm	C_2, F·cm	C_3, F·cm	-
$1.19\cdot10^{-7}$	$2.39\cdot10^{-3}$	$1.01\cdot10^{-1}$	-
α_1	α_2	α_3	-
0.81	0.63	0.19	-
θ_1 c	θ_2, º	θ_3, º	-
17.4	33.7	73.3	-
β_1, º	β_2, º	-	-
4.1	1.5	-	-

Thus, Θ = 17.4-73.3º, β < 4.1° indicates rather Cole-Cole representation for 10Sc1CeSZ ceramics obtained at 1250°C. In our previous work [23] where 10Sc1CeSZ obtained at higher temperatures was investigated it was shown that the Havriliak-Negami representation was observed for the samples with only one semicircle on impedance diagrams and the Cole-Cole representation was observed for two-semicircular graphs. For the first type of the samples the structure fragmentation disappeared. Thus as the deviation from Debye representation indicates higher degree of heterogeneity [10], we concluded that H-N representation clearly displays continuous monolithic microstructure where grain and grain boundary phase cannot be distinguished and give only one semicircle.

Conclusions

The method of electrical characterization of different components of solid oxide fuel cells depends on the porosity and content of metallic particles in the material. Such systems as anode or cathode can be successfully described by porous electrode theory (PET). Concerning the electrical characterization of solid electrolytes, the electrical impedance spectroscopy (EIS) is frequently used to separate the different contributions to the electrical resistivity. Impedance spectroscopy provides useful information in addition to the dc techniques regarding to the microstructure evolution of SOFC electrolyte materials: IS can provide more detailed information about percolation parameters (critical volume fraction and critical exponent), electrical degradation, effect of stabilizer, etc. While modeling of microstructure of composites with Debye response is simple and clear enough, electrical characterization of non-Debye systems provide the additional information about the degree of heterogeneity of the structure. However, as most of today's works elide this aspect of matter, we have not enough information concerning relaxation parameters for now.

Acknowledgements

Author wants to thank Dr. Oleksandr Vasylyev and Dr. Iegor Brodnikovsky from IPMS NASU for the given experimental data.

References

1. EG&G Technical Services, Inc. (2004), "Fuel Cell Handbook (Seventh Edition)". Office of Fossil Energy, National Energy Technology Laboratory. P. 427. Режим доступу: http://www.sofcpower.com/uploaded/documenti/fchandbook7.pdf.
2. Режим доступу: http://www.fuelcelltoday.com//about-fuel-cells/faq#2.
3. *Zhou X.-D., Singhal S. C.* (2009), "Fuel cells – solid oxide fuel cells". Encyclopedia of Electrochemical Power Sources, pp. 1–16.
4. *Nielsen J., Hjelm J.* (2014), "Impedance of SOFC electrodes: A review and a comprehensive case study on the impedance of LSM:YSZ cathodes". Electrochimica Acta. Vol. 115, pp. 31– 45.
5. *Paasch G., Micka K., Gersdorf P.* (1993), "Theory of the electrochemical impedance of macrohomogeneous porous electrodes". Electrochimica Acta. Vol. 38, pp. 2653–2662.
6. *Sonn V., Leonide A., Ivers-Tiffee E.* (2008), "Combined Deconvolution and CNLS Fitting Approach Applied on the Impedance Response of Technical Ni/8YSZ Cermet Electrodes". Journal of the Electrochemical Society. Vol. 155, B675.
7. *Mizutani Y.* (1994), "Development of high-performance electrolyte in SOFC". Solid State Ionics. Vol. 72, pp. 271–275.
8. *Badwal S., Ciacchi F., Milosevic D.* (2000), "Scandia–zirconia electrolytes for intermediate temperature solid oxide fuel cell operation". Solid State Ionics. Vol. 136, pp. 91–99.
9. *Omar S.* (2010), "Ionic conductivity ageing investigation of 1Ce10ScSZ in different partial pressures of oxygen". Solid State Ionics. Vol. 184 (1), pp. 2–5.
10. *Fonseca F. C., Mucillo R.* (2004), "Impedance spectroscopy analysis of percolation in (yttria-stabilized zirconia)-yttria ceramic composites". Solid State Ionics. Vol. 166, pp. 157-165.
11. *Alim M. A., Bissel S. R., Mobasher A. A.* (2008), "Analysis of the AC electrical data in the Davidson-Cole dielectric representation". Physica B. Vol. 403, pp. 3040-3053.
12. *Kleitz M., Steil M. C.* (1997), "Microstructure blocking effects versus effective medium theories in YSZ". J. Eur. Ceram. Soc. Vol. 17, Is. 6, pp. 819-829.
13. *Steil M. C., Thevenot F., Kleitz M.* (1997), "Densification of yttriastabilised zirconia: Impedance spectroscopy analysis". Journal of the Electrochemical Society. Vol. 144, pp. 390–398.
14. *Gerhardt R.* (1986), "Grain-boundary effect in ceria doped with trivalent cations: I. Electrical measurements". Journal of the American ceramic society. Vol. 69, №. 9, pp. 641-646.
15. *Guo X.* (2002), "Role of space charge in the grain boundary blocking effect in doped zirconia". Solid State Ionics. Vol. 154, pp. 555–561.
16. *Carvalho T.* (2012), "Lanthanum oxide as a scavenging agent for zirconia electrolytes". Solid State Ionics. Vol. 225 (4), pp. 484–487.
17. *Sarat S., Sammes N., Smirnova A.* (2006), "Bismuth oxide doped scandia-stabilized zirconia electrolyte for the intermediate temperature solid oxide fuel cells". Journal of Power Sources. Vol. 160 (2), pp. 892–896.
18. *Lee J. H.* (2000), "Improvement of grain-boundary conductivity of 8 mol% yttria-stabilized zirconia by precurs or scavenging of siliceous phase". Journal of the Electrochemical Society. Vol. 147 (7), pp. 2822–2829.
19. *Guo C. X., Wang J. X., He C. R.* (2013), "Effect of alumina on the properties of ceria and scandia co-doped zirconia for electrolyte-supported SOFC". Ceramics International. Vol. 39, pp. 9575–9582.

20. *Steele B. C. H., Heinzel A.* (2001), “Materials for fuel-cell technologies”. Nature. Vol. 414, pp. 345–352.
21. *Omar S., Najib W. B., Bonanos N.* (2011). “Conductivity ageing studies on 1M10ScSZ (M4+=Ce, Hf)”. Solid State Ionics. Vol. 189, pp. 100–106.
22. *McLachlan D. S.* (2007), “The AC and DC Conductivity of Nanocomposites” Journal of Nanomaterials. Vol. 2007, pp. 1-9.

Поступила в редакцию 20 сентября 2014 г.

УДК 53.097

І.В. Бродніковська, канд. техн. наук
Інститут проблем матеріалознавства ім. І. М. Францевича НАН України,
вул. Кржижановського, 3, 03680, Київ, Україна.

Дослідження електролітів ТОПЕ методами імпедансної спектроскопії (огляд)

У статті розглянуто різницю між методами електричної характеризації електродів і електролітів твердо-оксидних паливних елементів. Наведено особливості і можливості застосування ІС до матеріалів електролітів ТОПЕ з дебаєвським відгуком. Проведено комплексне вивчення можливих механізмів недебаєвської релаксації в матеріалах ТОПЕ. На прикладі експериментального вивчення кераміки 10Sc1CeSZ було проведено визначення мікроструктурних параметрів у випадку недебаєвського відгуку. Бібл. 22, рис. 8, табл. 2.

Ключові слова: *твердо-оксидні паливні елементи (ТОПЕ); електроліт; електрична характеризація; імпедансна спектроскопія; дебаєвський і недебаєвський відгук.*

УДК 53.097

И.В. Бродниковская, канд. техн. наук
Институт проблем материаловедения им. И. Н. Францевича НАН Украины,
ул. Кржижановского, 3, 03680, Киев, Украина.

Исследование электролитов ТОТЭ методами импедансной спектроскопии (обзор)

В статье рассмотрена разница между методами электрической характеризации электродов и электролитов твердо-оксидных топливных элементов. Приведены особенности применения ИС к материалам ТОТЭ с дебаевским откликом. Проведено комплексное изучение возможных механизмов недебаевской релаксации в материалах ТОТЭ. На примере экспериментального изучения керамики 10Sc1CeSZ было проведено определение микроструктурных параметров в случае недебаевского отклика. Библ. 22, рис. 8, табл. 2.

Ключевые слова: *твердо-оксидные топливные элементы (ТОТЭ); электролит; электрическая характеризация; импедансная спектроскопия; дебаевский и недебаевский отклик.*

Список использованных источников

1. Fuel Cell Handbook (Seventh Edition) by EG&G Technical Services, Inc. - U.S. Department of Energy, Office of Fossil Energy, National Energy Technology Laboratory, 2004 – 427 p. Режим доступу: http://www.sofcpower.com/uploaded/documenti/fchandbook7.pdf.
2. Режим доступу: http://www.fuelcelltoday.com/about-fuel-cells/faq#2.
3. *Zhou X.-D., Singhal S. C.* Fuel cells – solid oxide fuel cells // Encyclopedia of Electrochemical Power Sources. – 2009. – P. 1–16.

4. *Nielsen J., Hjelm J.* Impedance of SOFC electrodes: A review and a comprehensive case study on the impedance of LSM:YSZ cathodes // Electrochimica Acta. – 2014. – Vol. 115. – P. 31– 45.
5. *Paasch G., Micka K., Gersdorf P.* Theory of the electrochemical impedance of macrohomogeneous porous electrodes // Electrochimica Acta. – 1993. – Vol. 38. – P. 2653–2662.
6. *Sonn V., Leonide A.,* Ivers-Tiffee E. Combined Deconvolution and CNLS Fitting Approach Applied on the Impedance Response of Technical Ni/8YSZ Cermet Electrodes // Journal of the Electrochemical Society. – 2008. – Vol. 155. - B675.
7. *Mizutani Y.* Development of high-performance electrolyte in SOFC // Solid State Ionics. – 1994. – Vol. 72. – P. 271–275.
8. *Badwal S., Ciacchi F., Milosevic D.* Scandia–zirconia electrolytes for intermediate temperature solid oxide fuel cell operation // Solid State Ionics. – 2000. – Vol. 136. - P. 91–99.
9. *Omar S.* Ionic conductivity ageing investigation of 1Ce10ScSZ in different partial pressures of oxygen // Solid State Ionics. – 2010. – Vol. 184 (1). – P. 2–5.
10. *Fonseca F. C., Mucillo R.* Impedance spectroscopy analysis of percolation in (yttria-stabilized zirconia)-yttria ceramic composites // Solid State Ionics. – 2004. - Vol. 166. – P. 157-165.
11. *Alim M. A., Bissel S. R., Mobasher A. A.* Analysis of the AC electrical data in the Davidson-Cole dielectric representation // Physica B. – 2008. – Vol. 403. – P. 3040-3053.
12. *Kleitz M., Steil M. C.* Microstructure blocking effects versus effective medium theories in YSZ // J. Eur. Ceram. Soc. – 1997. – Vol. 17, Is. 6. – P. 819-829.
13. *Steil M. C., Thevenot F., Kleitz M.* Densification of yttriastabilised zirconia: Impedance spectroscopy analysis // Journal of the Electrochemical Society. – 1997. – Vol. 144. – P. 390–398.
14. *Gerhardt R.* Grain-boundary effect in ceria doped with trivalent cations: I. Electrical measurements // Journal of the American ceramic society. – 1986. – Vol. 69, №. 9. – P. 641-646.
15. *Guo X.* Role of space charge in the grain boundary blocking effect in doped zirconia // Solid State Ionics. – 2002. – Vol. 154. – P. 555–561.
16. *Carvalho T.* Lanthanum oxide as a scavenging agent for zirconia electrolytes // Solid State Ionics. – 2012. – Vol. 225 (4). – P. 484–487.
17. *Sarat S., Sammes N., Smirnova A.* Bismuth oxide doped scandia-stabilized zirconia electrolyte for the intermediate temperature solid oxide fuel cells // Journal of Power Sources. – 2006. – Vol. 160 (2). – P. 892–896.
18. *Lee J. H.* Improvement of grain-boundary conductivity of 8 mol% yttria-stabilized zirconia by precurs or scavenging of siliceous phase // Journal of the Electrochemical Society. – 2000. – Vol. 147 (7). – P. 2822–2829.
19. *Guo C. X., Wang J. X., He C. R.* Effect of alumina on the properties of ceria and scandia co-doped zirconia for electrolyte-supported SOFC // Ceramics International. – 2013. – Vol. 39. – P. 9575–9582.
20. *Steele B. C. H., Heinzel A.* Materials for fuel-cell technologies // Nature. – 2001. – Vol. 414. – P. 345–352.
21. *Omar S., Najib W. B., Bonanos N.* Conductivity ageing studies on 1M10ScSZ (M4+=Ce, Hf) // Solid State Ionics. – 2011. – Vol. 189. P. 100–106.
22. *McLachlan D. S.* The AC and DC Conductivity of Nanocomposites // Journal of Nanomaterials. – 2007. – Vol. 2007. – P. 1-9.